IEEJ Journal of Industry Applications
Vol.5 No.2 pp.123–131 DOI: 10.1541/ieejjia.5.123

Paper

A Nonlinear Adaptive Compliance Controller for Rehabilitation

Davide Pilastro* Non-member, Roberto Oboe*,** Non-member
Tomoyuki Shimono*** Member

(Manuscript received May 22, 2015, revised Nov. 13, 2015)

In the last few decades, the increase in the worldwide elderly population and the progress in the treatment of severe and chronic pathologies have led to a growing demand for rehabilitation therapies. Meanwhile, rehabilitation robotics has started to grow and to evolve, in order to develop suitable robotics devices and control strategies to better assist patients during training and to promote rehabilitation processes. In particular, some control strategies are designed to assist patients in completing the desired movements while applying the minimum force necessary. As a result, an "assist-as-needed" behavior can be achieved.

A novel nonlinear adaptive compliance controller, that aims to achieve such "assist-as-needed" behavior, has been developed and is presented in this paper. In addition to promote the active participation of patients, the proposed control also provides a tool to estimate and evaluate patient's state and therapeutic improvements. The proposed controller is obtained by appropriately merging a PD (proportional and derivative) control and an adaptive learning control. The latter is driven by the errors made by patients while performing the assigned exercise. As a result, the PD controller parameters are adapted according to different patient injuries and degrees of impairments and may be used to evaluate the improvements during training sessions. The paper presents an overview of the novel control algorithm and some preliminary clinical trials with real patients, demonstrating benefits of the controller.

Keywords: rehabilitation robotics, adaptive control

1. Introduction

In the last few decades, the increase of the worldwide elderly population and the progresses in the treatment of severe and chronic pathologies, like strokes, neurologic injuries and muscoloskeletal disorders, have led to a growth of the demand for rehabilitation therapies [1].

Indeed, such trend is sustained and promoted by several scientific studies showing how the plasticity of the human nervous system can be better exploited in relearning simple movements and regaining everyday life skills, if patients perform more therapies and treatments. In particular, this is a clear evidence in stroke patients, where it is also very important the timeliness in performing such rehabilitation therapies as soon as possible, after the acute events. So, it is easily understandable how the amount of recovery is closely linked to the amount and frequency of trainings and practices [2]–[4].

Even if benefits of rehabilitation therapies are already proved, there are some limitations in making them available to all those who need them. Such drawbacks are related to high costs and limited human resources, concerned with rehabilitation treatments.

In order to overcome these problems, in the last years a new field of research, called rehabilitation robotics, has started to grow and to evolve, in order to develop suitable robotic devices and control strategies to better assist patients during training and promote the rehabilitation processes. A number of research projects in the field of robotics and bioengineering have been launched, with the main purpose of designing and testing robotic devices and haptic interfaces, to be used in rehabilitation [5]–[9].

In this work, a typical robotic rehabilitation system will be considered, in which the patient interacts with a N-degrees of freedom (d.o.f.) robotic device, which is also interfaced to a VR environment. In this setting, a common rehabilitation task consists in asking the patient to follow a moving target, displayed in the VR environment, by properly moving the robot end-effector (see Fig. 1). Usually, the target movement repeatedly follows a specific trajectory, defined by the therapist.

The use of such kind of stand-alone robotic devices, combined with virtual reality (VR) tools, which help to keep the

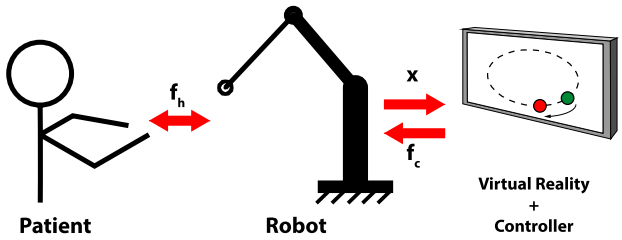

Fig. 1. Schematic representation of a typical stand-alone robotic rehabilitation system and related therapy

* University of Padova – Department of Management and Engineering
Stradella San Nicola, 3, 36100 Vicenza, Italy
** Fondazione Ospedale San Camillo I.R.C.C.S.
Via Alberoni, 70 - 30126 Venezia-Lido, Italy
*** Faculty of Engineering, Yokohama National University
79-5, Tokiwadai, Hodogaya, Yokohama 240-8501, Japan

patient involvement high, are becoming a common approach in the rehabilitation robotics. In fact, they can be a suitable solution to alleviate the previously mentioned problems, related to rehabilitation treatments. Indeed, they may allow to perform therapies directly at patient home. In addition, they can provide objective information about rehabilitation process to doctors and therapists, who, in this way, can check improvements.

In order to be used as stand-alone devices, without the supervision of specialized staff, the robotic rehabilitation systems must be able to adapt their action according to different patients and types and degrees of impairment. In particular, they must guarantee an active participation of patients during treatment, avoiding their slacking behaviors and better promoting rehabilitation process. To obtain this, the the controllers of the robots must be designed in order to provide assistance to the patient only when it is actually needed.

In the literature, it is possible to find many different control solutions to achieve such "assist-as-needed" behavior. In particular, such goal can be achieved in a very simple but not really effective fashion, by using position and impedance controllers with constant control parameters [10]–[12]. Another solution is based on the use of controllers with a triggered assistance. In such case, the robotic assistance starts when a specific performance variable reaches a threshold. The triggering variable could be participant's interaction force [13][14], the spatial tracking or speed error [15][16] or the muscle activity [17][18]. Lastly, the most convincing and promising solution is to implement performance-based adaptive controllers, where the control parameters or exercises to be performed are automatically tailored according to participant's impairments [19]–[25]. Unfortunately, previously described control strategies usually need additional sensors for their implementation (e.g. force or EMG sensors), leading to more complex and expensive devices.

Given that one of the goals we have set is to maintain the structure of the robotic device as simple and inexpensive as possible, we focused our attention on control strategies based exclusively on the use of "traditional" position sensors. In the literature, one solution to generate the required adaptive assistive force using only position sensors has been proposed in [26]. The main idea is to make use of an adaptive position-force map, which contains the value of the assistive force needed to bring the patient closer to the target position, for each point of the path to be followed. Such assistive force is provided in a feedforward fashion, so there are no problems from the point of view of the control stability. However, this approach presents some limitations and drawbacks. In fact, during the execution of a repetitive task, it may happen that the patient perfectly follows the moving target in a location in which he/she has previously made large errors. In such a case, the feedforward compensation generates a force based on the previous errors and pushes the patient away from the target position. So, the feedforward compensation may apply wrong assistive forces, as patients don't always perform errors in the same way. Furthermore, such control system does not always preserve the causal relationship between patient effort and resulting limb movements. Instead, many research studies [10][27]–[29] have shown how a properly set robot compliance (which implements a clear causal relation between effort and movements), stimulates motor learning process, encouraging patient engagement and effort.

The above considerations has led to the development of a novel adaptive assistance control algorithm, which takes inspiration from [26]. As it will be explained later, the essential idea behind the proposed control strategy is based on the observation of the assistive strategy used by the therapists, who usually adapt their compliance to the patients' conditions, helping them to complete the desired movement. The proposed approach makes use of an adaptive PD controller, which allows to vary the mechanical impedance felt by patients while manipulating the robot end-effector. Hence, the supportive action, performed by the robot, can be adjusted to be more compliant when patients perform a good tracking. On the other hand, when patients perform big errors, the controller becomes harder, in order to better guide patients along the trajectory to be followed. Unlike the solution proposed in [26], the assistive force is generated in a feedback fashion, avoiding the previously described undesired behaviors. On the other hand, the feedback loop leads to a stability issue, which is not straightforward to prove.

The paper is organised as follows. Section 2 contains an overview of the nonlinear adaptive impedance controller algorithm. Section 3 and Sect. 5 explain the experimental setup and the performed rehabilitation trials, respectively. Some experimental results will be presented in Sect. 6. At the end, in Sect. 7 some final remarks will be reported.

2. Nonlinear Adaptive Compliance Controller

As already mentioned, the presented control algorithm has been developed for specific robotic rehabilitation applications (see Fig. 1). On the other hand, there are no limitations related to the design, mechanical structure and number of d.o.f. of the robot to be used, as such control algorithm can be easily applied to different types of robot.

A key feature of such controller is its capability to emulate the therapist behavior during trainings, providing the least assistance needed. At the same time, it also promotes an active participation of patients, driving them to better perform the tasks. Indeed, analyzing the current values of the variable control parameters, it is possible to obtain a tool to estimate and evaluate patient's state, checking for example fatigue states and therapeutic improvements.

A significant aspect of such control system is its simplicity. Since it is based on the tracking error, it does not require any additional sensors, except standard encoders or position sensors, normally integrated in the actuators. Doing so, it is possible to avoid the design of expensive and bulky robotic systems. As a result, it could obtain the best possible performances in terms of promoting patient rehabilitation with a simple and low-cost rehabilitation robot system design. This is one of the biggest challenge concerning the rehabilitation robotics in order to design a robot device which is suitable to perform therapies directly at patient home and, furthermore, to be within everybody's reach.

It is also worth noticing that, while other control techniques used in rehabilitation aim at recovering muscle tone and strength, the control strategy proposed in this paper mainly focuses on the motor recovery aspects, related to the proper muscle activation, with the final target of a relearn of some

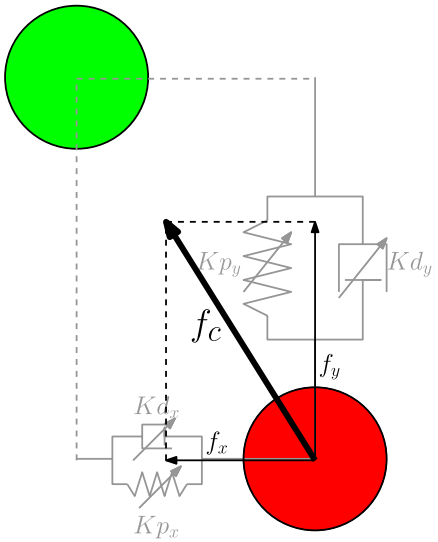

Fig. 2. Graphical representation of the adaptive compliance controller for a planar, 2-d.o.f. robot device

simple movements, to be used in everyday life.

2.1 Control Algorithm Going deeper into implementation details, the proposed approach is based on merging together an PD control and an adaptive learning control. Both control and adaptation strategies are inspired by the typical assistive action of the therapists, who tend to adapt their compliance to the tracking error of patients. In practice, a stiffer action is exerted on the patients in case they are not able to complete the desired movement, while the support is softer in case they are able to complete the proposed task autonomously. Such behavior better promote rehabilitation, as there is an active participation of the patient, who tries to properly activate his/her muscles.

The proposed controller solution provides an assistive action which approximates such therapist behaviors, simulating N viscoelastic elements, each of them independently acting along one of the workspace coordinates (see Fig. 2). The equilibrium point of each virtual spring coincide with the overlap of the red ball (end-effector) with the green ball (target to be followed). Thus, the control generates a variable attractive force $\mathbf{f_c}$ towards the target, as sum of individual forces, one for each d.o.f. (e.g. $\mathbf{f_x}$, $\mathbf{f_y}$ in Fig. 2 for planar, 2-d.o.f. robot case).

Moreover, the corresponding physical parameters of such virtual elements, (stiffness $K_{p_1} \dots K_{p_N}$ and viscosity $K_{d_1} \dots K_{d_N}$) are variable, depending on patient weakness, which is determined by evaluating his/her tracking performances. Clearly, due to specific patient's impairments, the tracking error may vary along the target trajectory to be followed and the degree of assistance should change accordingly. Roughly speaking, higher impedance gains are set in workspace locations where patients perform bigger errors. As a result, the proposed controller is implemented as N independent nonlinear functions of the N kinematic variables, which relates each point of the workspace to a specific set of controller proportional and derivative gains. Additionally, as will be explained later, such impedances are adapted over time, in order to follow any patient's performance variations.

The strict connection between controller gain values and patient's performances is clear. As a result, such correspondence allows to obtain some synthetic and easy to understand data, to constantly monitor patients during trainings. In fact, the observation of the virtual visco-elastic element values and their trends actually provide information related, for example, to patient's current state, e.g. fatigue or performance improvements.

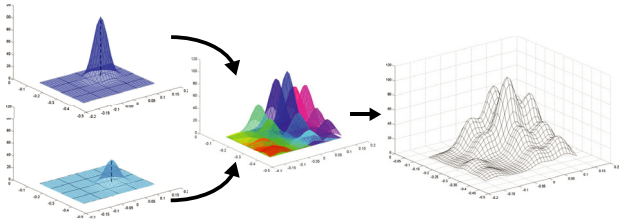

Fig. 3. Schematic representation of the approximation process of a nonlinear function, through the use of radial basis functions (RBFs) with Gaussian kernels

For the sake of simplicity, let's start the control algorithm explanation by analyzing, at first, the issue of representing a nonlinear function of N variables in a computationally efficient way. Among all the possible solutions, the use of radial basis functions (RBFs) with Gaussian kernel is a common approach, allowing to obtain a simple and efficient representation of nonlinear functions. An approximation of a nonlinear function spread over the workspace, based on RBFs with Gaussian kernel, can be performed by dividing such workspace into P non-overlapping areas, and placing at the center of each of them a properly weighted Gaussian function. The number of areas P is chosen in order to get the best trade-off between a good approximation and excessive computational complexity. As it can be seen in Fig. 3, an approximation of a generic nonlinear function, in the workspace, can be obtained by the properly weighted sum of such gaussian functions.

In the presented control algorithm, just the current controller proportional gains k_{p_i} are obtained by computing the N stiffness map, which is approximated by RBFs, in the current end-effector position. At the same time, the controller derivative gains k_{d_i} are defined in order to obtain a constant damping factor of the PD controllers. This choice has been made in order to not increase too much the overall computational effort of the control system. As a result, the control parameters computation are obtained as follows:

$$\mathbf{k_p}(\mathbf{x}(t)) = [k_{p_1} \dots k_{p_N}]^T = \widehat{\mathbf{k_p}(\mathbf{x}(t))} = Y(\mathbf{x}(t))\mathbf{a} \quad \cdots\cdots \quad (1)$$

$$\mathbf{k_d}(\mathbf{x}(t)) = [k_{d_1} \dots k_{d_N}] = \left[\frac{\xi}{2}\sqrt{k_{p_1}} \dots \frac{\xi}{2}\sqrt{k_{p_N}}\right] \quad \cdots\cdots \quad (2)$$

$$\mathbf{a} = [k_{p_{11}} \dots k_{p_{1P}}, k_{p_{21}} \dots k_{p_{2P}}, \dots, k_{p_{N1}} \dots k_{p_{NP}}]^T \quad \cdots\cdots\cdots\cdots\cdots\cdots \quad (3)$$

where $\mathbf{a}$ is a NP vector with the gaussian heights for the stiffness map approximations $\widehat{\mathbf{k_p}(\mathbf{x}(t))}$ and ξ is a constant damping factor of the controller, defined experimentally, while $\mathbf{Y}(\mathbf{x}(t))$ is a $N \times NP$-dimensional Gaussian weight matrix evaluated in the current end-effector location $\mathbf{x}(t)$, defined as follows:

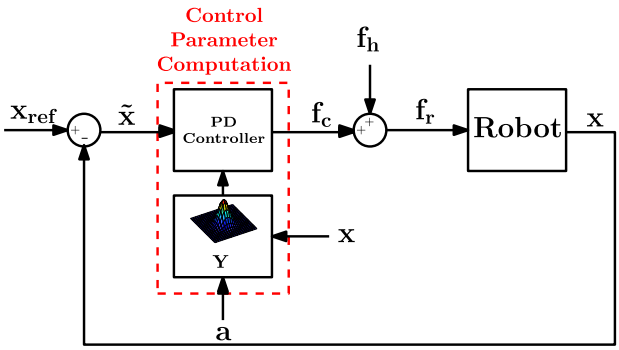

Fig. 4. Block diagram of the nonlinear compliance control system, showing how its control gains are varying according to the end-effector position and depending on vector **a** components

$$Y(\mathbf{x}) = \begin{bmatrix} g_1 \dots g_P & \mathbf{0} & \mathbf{0} \\ \mathbf{0} & \ddots & \mathbf{0} \\ \mathbf{0} & \mathbf{0} & g_1 \dots g_P \end{bmatrix} \quad \cdots\cdots\cdots\cdots\cdots (4)$$

$$g_i = \frac{c}{2\pi\sqrt{\det \boldsymbol{\Sigma}}} e^{-\frac{1}{2}(\mathbf{x}-\mu_i)^T \boldsymbol{\Sigma}^{-1}(\mathbf{x}-\mu_i)} \quad \cdots\cdots\cdots\cdots\cdots (5)$$

$$\sum_{i=1}^{P} g_i \leq 1 \quad \cdots\cdots\cdots\cdots\cdots\cdots\cdots\cdots\cdots\cdots (6)$$

where $\mu_\mathbf{i}$ is the center position of the i-th areas of the workspace, $\boldsymbol{\Sigma}$ is the $N \times N$-dimensional covariance matrix of the Gaussian bell and c is a normalizing gain, chosen in order to satisfy condition (6).

The amplitude of the Gaussian function bell depends on the values of the covariance matrix $\boldsymbol{\Sigma}$. It is advisable to set such values depending on the shape and size of the areas in which the workspace has been divided, in order to obtain a properly smooth approximated curve. A similar smooth result can be found in the control parameters variation.

An PD controller, with varying control parameters according to the current end-effector position, has been implemented in the control loop (see Fig. 4). As a result, the dynamic equation of a generic robot device is:

$$\mathbf{f_r}(\mathbf{x}(t), \tilde{\mathbf{x}}(t), \dot{\tilde{\mathbf{x}}}(t), t) = \mathbf{f_h}(t) + \mathbf{f_c}(\tilde{\mathbf{x}}(t), \dot{\tilde{\mathbf{x}}}(t), \mathbf{x}(t)) \cdots\cdots (7)$$

where $\mathbf{x}$, $\tilde{\mathbf{x}}$ and $\dot{\tilde{\mathbf{x}}}$ are respectively the N-dimensional current end-effector position vector and position and velocity error vectors ($\tilde{\mathbf{x}}(t) = \mathbf{r}(t) - \mathbf{x}(t)$ where $\mathbf{r}(t)$ is the target position), $\mathbf{f_h}$ is the human interaction force and $\mathbf{f_c}$ is the control force that assists the patient in completing the desired movements and defined by:

$$\mathbf{f_c}(\tilde{\mathbf{x}}(t), \dot{\tilde{\mathbf{x}}}(t), \mathbf{x}(t)) = K_p(\mathbf{x}(t))\tilde{\mathbf{x}}(t) + K_d(\mathbf{x}(t))\dot{\tilde{\mathbf{x}}}(\mathbf{t}) \quad \cdots\cdots\cdots\cdots\cdots (8)$$

$$K_p(\mathbf{x}(t)) = diag(\mathbf{k_p}(\mathbf{x}(t))) \quad \cdots\cdots\cdots\cdots\cdots\cdots (9)$$

$$K_d(\mathbf{x}(t)) = diag(\mathbf{k_d}(\mathbf{x}(t))) \quad \cdots\cdots\cdots\cdots\cdots (10)$$

2.2 Update Law In order to follow patients' improvements or changes in their weakness, the control algorithm implements also an adaptation of vector **a**, which defines the stiffness maps of controllers accordingly.

Indeed, the adaptation of **a** is the main aspect of the proposed control solution and, in this paper, it is proposed to make use of the following update law:

$$\dot{\mathbf{a}}(t) = \overbrace{-\frac{1}{\tau}\mathbf{Y}^T(\mathbf{Y}\mathbf{Y}^T)^{-1}\mathbf{Y}\mathbf{a}(t)}^{\text{forgetting term}} + \overbrace{k\mathbf{Y}^T abs(\tilde{\mathbf{x}}(\mathbf{t}))}^{\text{error term}} \quad \cdots\cdots (11)$$

$$\mathbf{a}(0) = \alpha_0[1 \dots 1]^T \cdots\cdots\cdots\cdots\cdots\cdots\cdots\cdots (12)$$

where α_0 is an arbitrary initial positive weight value and, for the sake of readability, position and error dependencies are omitted ($\mathbf{a}(t) = \mathbf{a}(t, \mathbf{x}(t), \tilde{\mathbf{x}}(t))$ and $\mathbf{Y} = \mathbf{Y}(\mathbf{x}(t))$).

The update law (11) consists of two terms:

- *forgetting term*: if no errors are performed, this term leads to an exponential decay of the parameters of **a**, with a time constant τ. The decrease of these parameters is weighted more in those areas closer to the current end-effector position, thanks to the matrix **Y**;
- *error term*: takes into account of errors performed by patients. Large errors cause large increases of the components of **a**, corresponding to areas which are close to the location where these errors are performed. k is a positive gain and by varying its value it is possible to change the error sensitivity of the update law. It is worth noticing that in (11), the absolute value of error is used in updating **a**. In this way, we account only for the error amplitude and not for its direction. This because patients do not perform errors always in the same direction. A direct consequence of an augmented **a** is the increase of the overall stiffness of the controllers in specific locations, as required.

As a consequence of the updating of **a**, the control parameters in (1) do not depend on the current end-effector position only, but they may also be updated over time, in order to keep memory of the patient performance history at different working positions. In fact, as long as small errors are performed, the first term of (11) results dominant and determines a decrease of the parameters while, when great errors occur, the dominant term becomes the second, causing an increment of the parameters and, in turn, of the controller stiffness at the position considered. As a result, the latter update law allows to take memory of the history performances of patients, over the workspace.

The differential equation in (11) has been discretised, in order to be digitally implemented. So, at each sampling time, the vector **a** is updated and the control stiffnesses are computed as follows:

$$\mathbf{k_p}(\mathbf{x}(t), t) = \mathbf{Y}(\mathbf{x}(t))\mathbf{a}(t) \cdots\cdots\cdots\cdots\cdots\cdots\cdots (13)$$

From (13) and using (2), the current derivative control gains are also updated. Lastly, the assistive force is obtained using (8), (9), (10). It is worth noticing that, given the adaptation mechanism implemented, the proportional and derivative gains vary according to the current end-effector position and also over time. The overall control system is shown in Fig. 5, where it can be clearly seen how the controller works in feedback fashion and how such controller is adapted.

Different behaviors of the adaptive control can be achieved by properly set values of τ and k parameters. In particular, regarding the forgetting factor τ, if an high value is chosen only slow changes in the patient's performance are followed. On the other hand, choosing a small value of τ allows a better tracking of the patient's performances, although obtaining

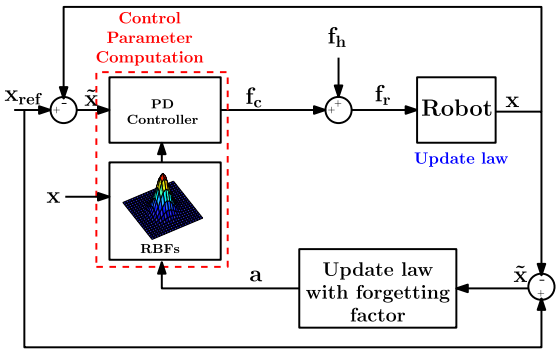

Fig. 5. Block diagram of the nonlinear compliance control system, really implemented. Compered to block diagram in Fig. 4, vector **a** is time-varing

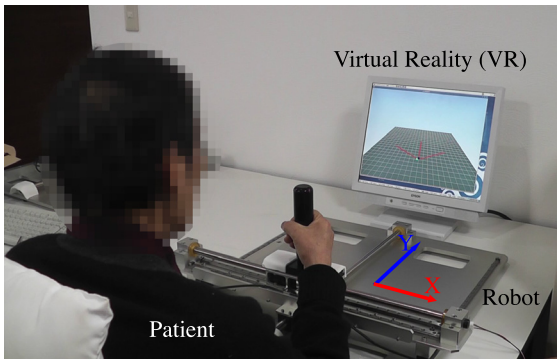

Fig. 6. Overview of the experimental setup and a typical rehabilitation trial

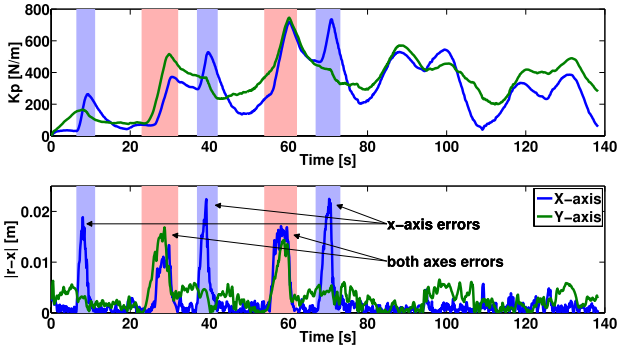

Fig. 7. Comparison between current proportional control gains and absolute position error, during a demo training with an healthy subject. Simulated tracking errors are performed during the first half of the trial, then accurate tracking is performed

noisier values of the controller parameters. The choice of the values for k, instead, directly determines the sensibility of the update law to the errors. An important issue is the choice of the initial value α_0, which is left to the therapist's decision. In fact, setting $\alpha_0 = 0$ leads to an absence of robotic assistance, at least at the beginning of the trial. Thereby, patients are encouraged, at first, to complete the exercise by themselves. On the other hand, when setting α_0 to a high positive value, the robotic assistance allows to correctly perform the task immediately, so the robot can teach the right movements to the participants. This could be very useful in case of patients with low cognitive skills. In both cases, anyhow, the update law leads to the right level of assistance, during the trails.

At the end of the control algorithm explanation, it is possible to understand its overall time-varying and nonlinear nature. Indeed, the previous mentioned update law parameters, τ and k are tunable by therapists themselves, in order to change the control behavior according to patients characteristics or type of training. For all these reasons, a control stability proof is needed, in particular to check the need boundaries in the update law parameters. A sketch of such proof is proposed in Appendix 1.

3. Experimental Setup

The presented adaptive control has been implemented in a rehabilitation robot system, designed to realize an haptic bilateral interface [30]. Nevertheless, the proposed application only makes use of one of the two sides of the bilateral system. This consists of a X-Y-table system with two d.o.f (see Fig. 6). Each axis is driven by a direct-drive linear motor with a optical encoder as position sensor. Such design is characterized by low friction losses and good back-drivability, allowing to realize accurate force control. The motion range of X-Y table is approximately 40 cm×40 cm. A grip rod is installed at the end effector of the robot, in order to facilitate the patient's gripping.

The motors are connected to their drivers, which are interfaced to a Linux computer through the use of a DAC board and a counter board for I/O signals. A user-friendly virtual reality (VR) environment has been implemented in the Linux system. A simple reaching task, that will be explained in Sect. 5, has been programmed. The use of VR allows to keep patient involvement high, providing a visual feedback, during the training. For further details about the overall system please refer to the related paper [30].

As seen in Fig. 8, the workspace area has been divided in a 6×6 matrix of equal squares. So, the number P of non-overlapping areas has been set to 36. Such choice has been made in order to limit the computation time, avoiding it exceeds the control sampling time, set to 1 ms.

4. Preliminary Tests

For the sake of better understanding how the control algorithm works, a preliminary test has been performed on an healthy subject. Specifically, he has been asked to follow a moving target on a circular trajectory. At first, the participant simulated a bad tracking, performing errors along a single axis or both axes, at the same time, and always in the same specific location of the trajectory to be followed. Then, accurate tracking has been performed.

Clearly, such experimental test wants to show the adaptive behavior of the controller. In fact, the so-called "assist-as-needed" behavior is shown in Fig. 7. As explained in Sect. 2, the control stiffness is adapted according patient's weaknesses. When a poor tracking of the target is performed, the controller tends to become harder. On the contrary, when a good tracking is achieved, the controller becomes softer, decreasing the total assistive force. Graphs in Fig. 7 are time-varying, but, since the target is moving, stiffness variations are located only in neighborhood of current end-effector position and also taking into account of the performance history

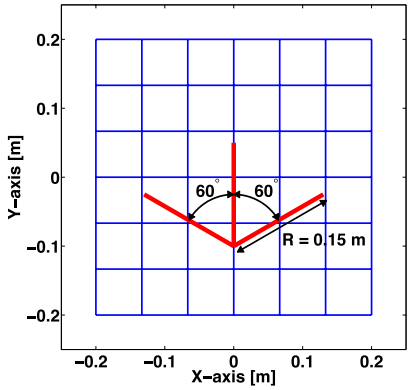

Fig. 8. Schematic representation of the workspace partition and the path to be followed in the rehabilitation task. Length, directions and speed of the target have been decided by therapists

Table 1. Subjects involved in the trials

Subject #	1	2	3	4
Gender	Male	Male	Female	Female
Age	72	73	83	76
Disorder	Stroke	Stroke	Dementia	Parkinsonism
Affected side	Left	Right	-	-

in such specific workspace area. This is obtained thanks to the update law definition and the gaussian weights in the computation.

5. Rehabilitation Trials

In order to show the effectiveness of the proposed control system, some preliminary rehabilitation trials with patients have been performed.

Type of trials and schedule have been decided together with specialists and physiotherapists. The first rehabilitation task chosen for the tests was an easy reaching one. During trainings, subjects were encouraged to properly moving the robot end-effector, following a target which is repeatedly moving back and forth in three different directions (see Fig. 8). The resulting movement somehow emulates a common and useful daily-life activity of reaching some objects, placed in front of a person.

All tunable control parameters have been set by asking advices to therapists. In particular, in order to obtain a smooth adaptation of the controller, the update parameter τ and k have been set to 20 s and 500 N/m^2, respectively. At the same time, the controller has been initialized with $\alpha_0 = 10\,\mathrm{N/m}$, corresponding to a very soft stiffness of the controller. In such a way, at the beginning of the training, the robot assistance was minimized, encouraging patients to perform movements by themselves.

Four aged adults attended the trials. Two of them were chronic stroke patients while the other two were effected by middle-dementia and Parkinsonism, respectively (see Table 1). It's worth noting that the last two patients had no impairments in their limbs motions, while they were affected by low cognitive skills. This affected their ability in maintaining their attention focused on the task, during training.

Trials have been performed by the first two patients by using their stroke affected arm, while, the others have been using their dominant arm.

Table 2. Training schedule for a weekly session

Trial #	1	2	3	4	5
Controller computation	ON	ON	ON	ON	ON
Motor driver	OFF	ON	ON	ON	OFF

Each subject attended four rehabilitation sessions, once a week. Five trainings have been performed in each session. During each training, patients were asked to follow the moving target along the previously described reaching trajectory, repeating such movements for three times. Such task was completed in about 150 s (target speed has been set to 1.8 cm/s).

In order to better understand the benefits of the treatment, the five trainings were not all the same. In fact, the first and the last ones have been performed with disabled motors drives, as it can be seen in Table 2. In such cases, no force feedback has been sent to patients, allowing free movements. Nevertheless, the adaptive control algorithm was active, allowing the computation of the stiffness map over the workspace. So, some pre- and post- treatment performance information have been made available.

6. Experimental Results

During trials, current end-effector and reference positions, current control parameters and values of the NP gaussian heights for the N stiffness maps have been saved. So, a huge amount of data was obtained for each patient. However, to show the proposed solution advantages, in this paper, only data from two rehabilitation sessions, performed by one stroke (Subject-1) and one no-stroke (Subject-3) patient will be presented, respectively.

First of all, looking at free movement columns in Fig. 9, it is possible to understand how the proposed approach provides a tool to easily evaluate patient's degrees of impairment and locations where they are more significant. The colored graphs have been obtained by computing the controller stiffness map, from the last values of vector **a**, for each trial. Last values have been chosen, since they better summarized patient behavior during training, as the controller has time to correctly adapted its parameters. Red colored areas show low patient tracking performances, as stiffness is higher. Meanwhile, blue areas suggest good tracking performances, as the controller is soft. This relationship is also clear by observing averages and standard deviations of position errors in the Table 3. In fact, graphs characterized by bigger red areas show also higher absolute error average and standard deviation values. Compared to simple statistical data in Table 3, the graphs in Fig. 9 provide additional information about tracking performance distribution over the workspace. Such information can be very useful to therapists, in order to better understand and promote rehabilitation process. In fact, comparing first and last graphs in Fig. 9, therapists can check some patients improvements, as the red colored areas are smaller and less visible. Such evaluation can be executed in the active control training too. Here, therapists can obtain additional details, for example related to patient wearying (see active control graphs in Fig. 9, patient performances get worse in the fourth trial compared to previous ones).

Another key benefit, achieved by using the proposed

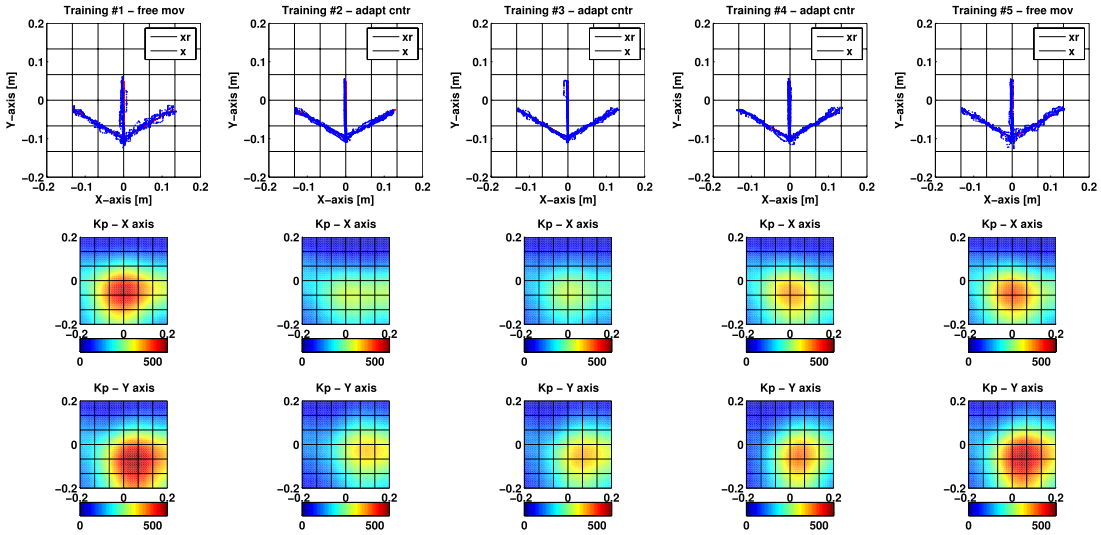

Fig. 9. Subject-1 (stroke patient): the figure shows three different graphs for each training in a session. First row compares reference position and end-effector position, sampled during trainings. Second and third row show the final stiffness impedance map for *X* and *Y* axes, respectively

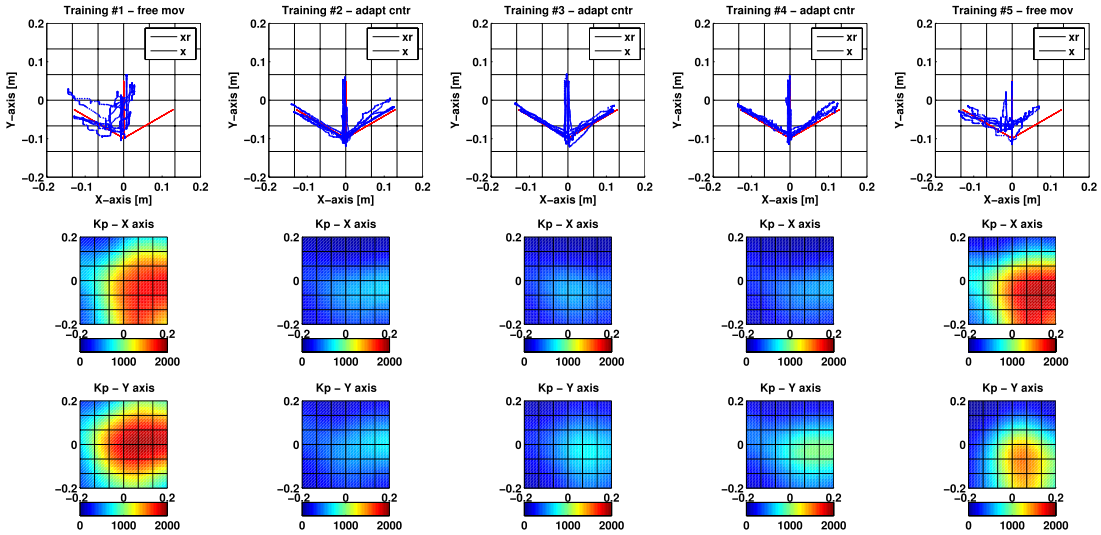

Fig. 10. Subject-3 (no-stroke patient): the figure shows three different graphs for each training in a session. First row compares reference position and end-effector position, sampled during trainings. Second and third row show the final stiffness impedance map for *X* and *Y* axes, respectively

Table 3. Subject-1 (stroke patient): mean absolute (MAE) and standard deviation (SD) error results

	X-axis		Y-axis	
trial #	MAE [mm]	SD [mm]	MAE [mm]	SD [mm]
1	5.45	5.66	5.19	4.73
2	3.96	4.41	2.93	3.64
3	3.34	4.01	3.38	2.92
4	4.16	4.46	3.75	3.89
5	4.57	5.50	3.94	4.74

Table 4. Subject-3 (no-stroke patient): mean absolute (MAE) and standard deviation (SD) error results

	X-axis		Y-axis	
trial #	MAE [mm]	SD [mm]	MAE [mm]	SD [mm]
1	28.94	29.71	28.39	25.20
2	7.28	8.86	5.57	6.71
3	6.41	7.64	4.50	6.28
4	6.56	9.26	5.83	5.96
5	25.59	19.36	26.29	19.71

control solution, is to promote the active participation of patient and keep his/her involvement high. This is an important issue in patients with low cognitive capabilities. Although some of such patients doesn't have physical impairments, they only need trainings to preserve muscle tone of their limbs. So, the assistive force is merely helpful to better teach tasks to these patients and correctly complete their movements. Figure 10 shows some results performed by a patient affected by middle-dementia. The clear discrepancy in the performance results between the inactive and active control trainings is proving the previous mentioned control benefits. Such result is also confirmed by numerical data in Table 4. During active-control trails, just a small assistive force was needed to correctly perform tasks, while in free movement trials tracking performances got strongly worse, showing how the visual feedback itself wasn't enough to achieve good performances.

7. Conclusions

A novel adaptive compliance controller for rehabilitation purposes has been presented in this paper.

Some preliminary clinical tests have been performed with real patients, in order to evaluate benefits of such control approach. In particular, the experimental results have shown its effective "assist-as-needed" behavior, which encourages the active participation of patient in the execution of tasks. Moreover, by properly analyzing the control parameters, it possible to obtain an useful patient's performance evaluation tool. In fact, it gives information about degree and location of patients' weaknesses.

Future works will concern the realization of a greater number of rehabilitation trails, in order to better prove its advantages in the rehabilitation process over a long time horizon.

Acknowledgment

The authors would like to thank Ms. Yuri Hasegawa and physical therapists at the "Kazenotani project" rehabilitation center in Miura, Kanagawa, Japan, for their support and collaboration. They also appreciate Prof. Shinichiro Ishii, a professor at Kanagawa University of Human Services for his valuable advice. Also, a special thanks go to patients who, kindly, participated in the trials.

References

(1) T.E.R. of Stroke (EROS) Investigators: "Incidence of stroke in Europe at the beginning of the 21st century", Stroke, Vol.40, No.5, pp.1557–1563 (2009)
(2) R.J. Nudo: "Mechanisms for recovery of motor function following cortical damage", Current Opinion in Neurobiology, Vol.16, No.6, pp.638–644 (2006)
(3) G. Kwakkel: "Impact of intensity of practice after stroke: Issues for consideration", Disability and Rehabilitation, Vol.28, No.13-14, pp.823–830 (2006)
(4) G. Kwakkel, B. Kollen, and J. Twisk: "Impact of time on improvement of outcome after stroke", Stroke, Vol.37, No.9, pp.2348–2353 (2006)
(5) H.I. Krebs, et al.: "Rehabilitation robotics: pilot trial of a spatial extension for MIT-Manus", Journal of NeuroEngineering and Rehabilitation, Vol.1, No.1 (2004)
(6) S. Masiero, A. Celia, G. Rosati, and M. Armani: "Robotic-Assisted Rehabilitation of the Upper Limb After Acute Stroke", Archives of Physical Medicine and Rehabilitation, Vol.88, No.2, pp.142–149 (2007)
(7) Lum, Peter S., et al.: "MIME robotic device for upper-limb neurorehabilitation in subacute stroke subjects: A follow-up study", Journal of rehabilitation research and development, Vol.43, No.5, p.631 (2006)
(8) A. Turolla, A.O. Daud Albasini, R. Oboe, M. Agostini, P. Tonin, S. Paolucci, G. Sandrini, A. Venneri, and L. Piron: "Haptic-based neurorehabilitation in poststroke patients: a feasibility prospective multicentre trial for robotics hand rehabilitation", Computational and mathematical methods in medicine (2013)
(9) T. Tsuji, Y. Hasegawa, Y. Sakurai, T. Yokoo, K. Abe, and S. Ishii: "Development of rehabilitation support robot with guidance control based on biarticular muscle mechanism", *IEEJ Trans. IA*, Vol.3, No.4, pp.350–357 (2014)
(10) H.I. Krebs, N. Hogan, M.L. Aisen, and B.T. Volpe: "Robot-aided neurorehabilitation", IEEE Trans. on Rehabilitation Engineering, Vol.6, pp.75–87 (1998)
(11) M.L. Aisen, et al.: "The effect of robot-assisted therapy and rehabilitative training on motor recovery following stroke", Archives of neurology, Vol.54, pp.443–446 (1997)
(12) L.L. Cai, et al.: "Implications of assist-as-needed robotic step training after a complete spinal cord injury on intrinsic strategies of motor learning", The Journal of neuroscience, Vol.26, pp.10564–10568 (2006)
(13) Loureiro, Rui CV, and W.S. Harwin: "Reach & grasp therapy: design and control of a 9-DOF robotic neuro-rehabilitation system", IEEE 10th International Conference on Rehabilitation Robotics (2007)
(14) J.-J. Chang, et al.: "Effects of robot-aided bilateral force-induced isokinetic arm training combined with conventional rehabilitation on arm motor function in patients with chronic stroke", Archives of Physical Medicine and Rehabilitation, Vol.88, pp.1332–1338 (2007)
(15) S.K. Banala, S.K. Agrawal, and J.P. Scholz: "Active Leg Exoskeleton (ALEX) for gait rehabilitation of motor-impaired patients", IEEE 10th International Conference on Rehabilitation Robotics (2007)
(16) L. Khan, et al.: "Robot-assisted reaching exercise promotes arm movement recovery in chronic hemiparetic stroke: A randomised controlled pilot study 6", Journal of NeuroEngineering & Rehabil, Vol.3, pp.1–13 (2006)
(17) J.C. Perry, J. Rosen, and S. Burns: "Upper-limb powered exoskeleton design", IEEE/ASME Transactions on Mechatronics, Vol.12, pp.408–417 (2007)
(18) L. Dipietro, et al.: "Customized interactive robotic treatment for stroke: EMG-triggered therapy", IEEE Trans. Neural Systems and Rehabilitation Engineering, Vol.13, pp.325–334 (2005)
(19) R. Riener, et al.: "Patient-cooperative strategies for robot-aided treadmill training: first experimental results", IEEE Trans. Neural Systems and Rehabilitation Engineering, Vol.13, pp.380–394 (2005)
(20) H.I. Krebs, et al.: "Rehabilitation robotics: Performance-based progressive robot-assisted therapy", Autonomous Robots, Vol.15, pp.7–20 (2003)
(21) L.E. Kahn, W.Z. Rymer, and D.J. Reinkensmeyer: "Adaptive assistance for guided force training in chronic stroke", the IEEE 26th Annual International Conference of Engineering in Medicine and Biology Society, Vol.1 (2004)
(22) D. Erol and N. Sarkan: "Intelligent control for robotic rehabilitation after stroke", Journal of Intelligent and Robotic Systems, Vol.50, pp.341–360 (2007)
(23) J. Von Zitzewitz, M. Bernhardt, and R. Riener: "A novel method for automatic treadmill speed adaptation", IEEE Trans. Neural Systems and Rehabilitation Engineering, Vol.15, pp.401–409 (2007)
(24) P. Kan, et al.: "The development of an adaptive upper-limb stroke rehabilitation robotic system", Journal of neuroengineering and rehabilitation, Vol.8, pp.1–18 (2011)
(25) E. Vergaro, et al.: "Self-adaptive robot training of stroke survivors for continuous tracking movements", J Neuroeng Rehabil, Vol.7, pp.1–12 (2010)
(26) E. Wolbrecht, V. Chan, D. Reinkensmeyer, and J. Bobrow: "Optimizing compliant, model-based robotic assistance to promote neurorehabilitation", IEEE Trans. Neural Systems and Rehabilitation Engineering, Vol.16, No.3, pp.286–297 (2008)
(27) R.A. Schmidt and T. Lee: "Motor control and learning", Human kinetics (1988)
(28) J.F. Israel, et al.: "Metabolic costs and muscle activity patterns during robotic-and therapist-assisted treadmill walking in individuals with incomplete spinal cord injury", Physical therapy, 86.11, pp.1466–1478 (2006)
(29) L.L. Cai, et al.: "Effects of consistency vs. variability in robotically controlled training of stepping in adult spinal mice", IEEE 9th International Conference on Rehabilitation Robotics, pp.1466–1478 (2005)
(30) C. Morito, T. Shimono, N. Motoi, Y. Fujimoto, T. Tsuji, Y. Hasegawa, K. Abe, Y. Sakurai, and S. Ishii: "Development of a haptic bilateral interface for arm self-rehabilitation", IEEE/ASME International Conference on Advanced Intelligent Mechatronics (AIM), pp.804–809 (2013)
(31) A.M. Lyapunov: "The general problem of the stability of motion", International Journal of Control, Vol.55, No.3, pp.531–534 (1992)
(32) J.-J.E. Slotine and W. Li: "Applied nonlinear control", NJ: Prantice-Hall, Englewood Cliffs (1991)
(33) E.J. Perreault, R.F. Kirsch, and A.M. Acosta: "Multiple-input, multiple-output system identification for characterization of limb stiffness dynamics", Biological cybernetics, Vol.80, No.5, pp.327–337 (1999)
(34) T. Tsuji, P.G. Morasso, K. Goto, and K. Ito: "Human hand impedance characteristics during maintained posture", Biological cybernetics, Vol.72, No.6, pp.475–485 (1995)
(35) K.P. Tee, E. Burdet, C.-M. Chew, and T.E. Milner: "A model of force and impedance in human arm movements", Biological cybernetics, Vol.90, No.5, pp.368–375 (2004)
(36) J. Palazzolo, M. Ferraro, H. Krebs, D. Lynch, B. Volpe, and N. Hogan: "Stochastic estimation of arm mechanical impedance during robotic stroke rehabilitation", IEEE Trans. Neural Systems and Rehabilitation Engineering, Vol.15, No.1, pp.94–103 (2007)

Appendix

1. Control Stability Proof

Due to the time-varying and nonlinear nature of the previously presented compliance controller and presence of a human force acting on the system, its stability proof has been carried out using an energetic approach, taking advantages of the Lyapunov theory [31][32].

In order to simplify the discussion, some proper constraints and model simplifications are defined:

- limited end-effector and target position and speeds:

$$\|\mathbf{x}(t)\|_\infty \leq x_{max} \quad , \quad \|\mathbf{r}(t)\|_\infty \leq r_{max} \cdots\cdots\cdots\cdots \text{(A1)}$$

$$\|\dot{\mathbf{x}}(t)\|_\infty \leq \dot{x}_{max} \quad , \quad \|\dot{\mathbf{r}}(t)\|_\infty \leq \dot{r}_{max} \cdots\cdots\cdots\cdots \text{(A2)}$$

- lower bounded stiffness of the N independent PD controllers, in order to prevent system from degenerating into an open loop one:

$$\|\mathbf{a}(t)\|_\infty \geq a_{min} > 0 \cdots\cdots\cdots\cdots\cdots\cdots\cdots\cdots \text{(A3)}$$

- human interaction force modelled as a second order linear model [33]–[36]:

$$\mathbf{f_h} = M_h\ddot{\mathbf{x}} + K_h\tilde{\mathbf{x}} + b_h\dot{\tilde{\mathbf{x}}} \cdots\cdots\cdots\cdots\cdots\cdots\cdots\cdots \text{(A4)}$$

with M_h, K_h, b_h, respectively, diagonal and positive-definite constant human mass matrix and impedance parameter matrices. Constant values for such parameters are set, as their changes, correlated to tracking performance improvements and motion recovery, are slower than the control dynamics. So, their variation effects can be neglected in the stability analysis.

The stability proof can be carried out in two steps: starting from a single d.o.f robot case and extending the results to a multi-d.o.f case.

1.1 Single d.o.f. Robot Device Using the 1-d.o.f. version of (7), (8) and (A4), the dynamic equation of such simple robot system can be written as:

$$m_r\ \ddot{x}(t) = m_h\ddot{x} + (K_p(t) + K_h)\tilde{x} + (K_d(t) + b_h)\dot{\tilde{x}} \cdots\cdots\cdots\cdots\cdots\cdots\cdots\cdots \text{(A5)}$$

where m_r, the manipulator mass, K_p and K_d and the human parameters are positive scalar values. (A5) can be rewritten as follows:

$$m_{tot}\ddot{x}(t) = -K_{tot}\tilde{x}(t) - b_{tot}\dot{\tilde{x}}(t) \cdots\cdots\cdots\cdots\cdots\cdots\cdots\cdots \text{(A6)}$$

where $m_{tot} = m_r + m_h$, $K_{tot} = K_p(t) + K_h$ and $b_{tot} = K_d(t) + b_h$. The Lyapunov function, used in the demonstration, takes into account of the total energy stored into the system, as follows:

$$V(t) = \overbrace{\frac{1}{2}m_{tot}(x)\dot{x}(t)^2}^{\text{kinetic energy}} + \overbrace{\frac{1}{2}K_{tot}(t)\tilde{x}(t)^2}^{\text{control energy}} \cdots\cdots\cdots\cdots\cdots\cdots \text{(A7)}$$

While, from the theory, the Lyapunov asymptotic stability condition is:

$$\dot{V}(t) < 0 \Rightarrow -2\,(K_p(t) + K_h)\frac{\dot{r}(t)}{\tilde{x}(t)} + \dot{K}_p(t) < 0 \cdots\cdots\cdots\cdots\cdots\cdots\cdots\cdots \text{(A8)}$$

Taking into account of K_p computation, the control update law (11) and previous defined constraints, such stability condition leads to the following boundaries:

$$k < \frac{a_{min}}{x_{max}}\left(\frac{1}{\tau} - \frac{v_{max}\ c\ P}{\sigma^2\sqrt{2\pi e}} - 2\,\frac{\dot{r}_{max}}{x_{max}}\right) - 2K_h\frac{\dot{r}_{max}}{x_{max}^2} \cdots\cdots\cdots\cdots\cdots\cdots\cdots\cdots \text{(A9)}$$

$$\tau < \frac{1}{\frac{v_{max}\ c\ P}{\sigma^2\sqrt{2\pi e}} + 2\,\frac{\dot{r}_{max}}{x_{max}} + 2K_h\frac{\dot{r}_{max}}{x_{max}a_{min}}} \cdots\cdots\cdots\cdots \text{(A10)}$$

Inequalities in (A9) and (A10) show how, in order to guarantee the asymptotic stability of the system, boundaries, in the maximum error sensitivity and in the minimum forgetting rate of the update law, are needed.

1.2 N d.o.f Robot Device In this case, it's better to simplify the proof, firstly consider no without human interaction force and no moving target. The dynamic equation of the robot system can be rewritten in the joint space ($\mathbf{q}(t)$, for better readability $\mathbf{q}$, is the joint space coordinate vector):

$$H_r(\mathbf{q})\ddot{\mathbf{q}} + C_r(\mathbf{q},\dot{\mathbf{q}})\dot{\mathbf{q}} = J_a(\mathbf{q})^T\left(-K_p(\mathbf{x}(t))\mathbf{x} - K_d(\mathbf{x}(t))\dot{\mathbf{x}}\right) \cdots\cdots\cdots\cdots\cdots\cdots \text{(A11)}$$

where J_a is the analytical Jacobian, while $H_r(\mathbf{q})$ is the inertia matrix in the joint space and $C_r(\mathbf{q},\dot{\mathbf{q}})$ is the Coriolis matrix of the manipulator. Also the Lyapunov function can be rewritten, as follows:

$$V = \overbrace{\frac{1}{2}\dot{\mathbf{q}}^T H_r(\mathbf{q})\dot{\mathbf{q}}}^{\text{kinetic energy}} + \overbrace{\frac{1}{2}\mathbf{x}^T K_p(\mathbf{x}(t))\mathbf{x}}^{\text{control energy}} \cdots\cdots\cdots\cdots\cdots\cdots \text{(A12)}$$

differentiating (A12) and using skew-symmetric property of matrix $\dot{H}_r - 2C_r$ the derivative of the Lyapunov function becomes:

$$\dot{V} = -\dot{\mathbf{x}}^T K_d(\mathbf{x}(t))\dot{\mathbf{x}}^T + \frac{1}{2}\mathbf{x}^T K_p(\mathbf{x}(t))\mathbf{x} \cdots\cdots\cdots\cdots\cdots\cdots \text{(A13)}$$

By noting that the right-hand side of (A13) is a quadratic form with diagonal matrices, the stability proof is straightforward. As, it is possible to split it in N independent 1-d.o.f. subproblems, one for each d.o.f. Also adding the human interaction force and the moving target is straightforward (see Appendix 1.1).

Davide Pilastro (Non-member) was born in Thiene, Italy, on December 8, 1988. He received the B.E., M.E. in mechatronics engineering from University of Padova, Padova, Italy, in 2010 and 2012, respectively. Currently, he is a Ph.D. student on mechatronics and product innovation engineering in the Department of Management and Engineering, Vicenza, Italy. His research interests include rehabilitation robotics, sensor fusion, and motion control.

Roberto Oboe (Non-member) was born in Lonigo, Italy, on October 26, 1963. He received the Laurea degree (cum laude) in electrical engineering and the Ph.D. degree from the University of Padova, Padova, Italy, in 1988 and 1992, respectively. He is presently Associate Professor of Automatic Control at the Department of Management and Engineering of the University of Padova, Vicenza, Italy. His research interests are in the fields of applied digital control, telerobotics, haptic devices, rehabilitation robots and applications and control of MEMS.

Tomoyuki Shimono (Member) received the B.E. degree in mechanical engineering from Waseda University, Tokyo, Japan, in 2004 and the M.E. and Ph.D. degrees in integrated design engineering from Keio University, Yokohama, Japan, in 2006 and 2007, respectively. He is currently an associate professor at Faculty of Engineering in Yokohama National University, Yokohama, Japan. His research interests include haptics, motion control, medical and rehabilitation robots, and actuators.